



86-GBaud subcarrier multiplexed 16QAM signal generation using an electrical 90 degree hybrid and IQ mixers

T. ZHANG,^{1,*} C. SANCHEZ,^{1,2} P. SKVORTCOV,¹ F. FERREIRA,¹ S. SYGLETOS,¹ I. PHILLIPS,¹ W. FORYSIAK,¹ AND A. ELLIS¹

¹Aston Institute of Photonic Technologies (AIPT), Aston University, Birmingham, B4 7ET, UK

²Airbus Defense and Space, Gunnels Wood Rd, Stevenage, SG1 2AS, UK

*zhangt16@aston.ac.uk

Abstract: We experimentally demonstrate an aggregate 86-GBaud (over three sub-bands and one polarization) signal generation based on subcarrier multiplexing technique using IQ mixers, an electrical 90 degree hybrid, and diplexers. The electrical hybrid allows transmitter-side digital signal processing to be simplified to pulse shaping and digital pre-emphasis. We verified the configuration by testing the performance of an 86-GBaud Nyquist-shaped 16 quadrature amplitude modulation signal with differential bit encoding. The implementation penalty assuming 7% hard-decision forward error correction is reduced to 2 dB by utilizing a 31-tap decision-directed least mean square based multiple-input multiple-output equalizer for sideband crosstalk mitigation.

Published by The Optical Society under the terms of the [Creative Commons Attribution 4.0 License](https://creativecommons.org/licenses/by/4.0/). Further distribution of this work must maintain attribution to the author(s) and the published article's title, journal citation, and DOI.

1. Introduction

Driven by the ever increasing requirement to transport more data, higher-speed (400 Gb/s or 1 Tb/s) optical interfaces are highly desirable. Optical super-channels [1–3], optical sub-bands multiplexing [4], multiple spectral slices synthesis multiplexing [5,6], and orthogonal optical time division multiplexing [7] have been introduced to realize terabit transmission. However, either a large number of parallel opto-electronic components or additional modulators for frequency-locked subcarriers generation are required, which inevitably increases transponder cost and complexity. Since transponder cost per bit generally decreases as data rates per opto-electronic conversion are increased, great efforts have been made to electrically generate high symbol rate signals in single carrier system with single optical modulator. The proposed electrical approaches mainly include analog-multiplexed digital to analogue converters (DACs) [8], all-DACs [9], electrical time-division multiplexing (ETDM) [10] and digital bandwidth interleaving [11], with generated signals of 80-GBaud four-level pulse amplitude modulation (PAM4), 105-Gaud probabilistic shaped 64-ary quadrature amplitude modulation (64QAM), 120-GBaud 16QAM, and 190-GBaud PAM4. Each technique offers its own unique features and drawbacks, and given recent progress for all options, no clear leading approach has yet been identified.

In this paper, we introduce another form of frequency multiplexing, adding IQ mixers and hybrid couplers in the radio frequency (RF) domain in order to simplify the transmitter-side digital signal processing (DSP), which enables simple RF oscillator suppression via DC offset optimization without sacrificing DAC resolution and eliminates joint sub-band processing in the transmitter. The proposed scheme also allows flexible choice of the RF oscillator frequency with the help of digital frequency shift and makes full use of the transmitter optical bandwidth by utilizing hybrid-assisted tandem single sideband (TSSB) modulation [12]. Specifically, we report an aggregate baud rate of 86 GBaud (over three sub-bands and one polarization) 16QAM signal generation based on subcarrier multiplexing (SCM) technique,

using passive RF components, single optical IQ modulator, and simplified transmitter-side DSP. The implementation penalty at the 7% hard-decision forward error correction (HD-FEC) threshold was effectively reduced to 2 dB, benefiting from a 31-tap decision-directed least mean square (DDLMS) based multiple-input multiple-output (MIMO) equalizer for inter sub-band crosstalk mitigation.

2. 86-GBaud SCM based transmitter

2.1 Principle

Figure 1 depicts the architecture of our SCM-based Nyquist shaped (roll-off factor of 0.05) 86-GBaud transmitter. The generated 86-GBaud optical signal can be sliced into three bands, i.e. lower sideband (LSB), baseband (BB) and upper sideband (USB) [see Fig. 1(k)]. Since the data for each band is independent, DACs with different sampling rates can be used. For the BB signal, 38-GBaud 16QAM data [-20 GHz to 20 GHz, Fig. 1(a)] is converted to analogue signals [Fig. 1(d) for quadrature] with two 32-GHz 8-bit 76-GSa/s DACs. 24-GBaud data streams for the LSB and USB are digitally frequency shifted by -1 GHz, with signal spectrum occupying from -13.6 GHz to 11.6 GHz in Figs. 1(b) and 1(c) before conversion to analogue signals through four 25-GHz 8-bit 64-GSa/s DACs. The generated in-phase and quadrature analogue signals with frequency range from -13.6 GHz to 13.6 GHz [see Figs. 1(e) and 1(f)] are then separately input to the IQ mixers with 33-GHz RF local oscillators for up-conversion. Due to -1 -GHz digital frequency shift, the up-converted electrical signals are centered at ± 32 GHz, occupying spectrum from 19.4 GHz to 44.6 GHz and from -44.6 GHz to -19.4 GHz [see Figs. 1(g) and 1(h)].

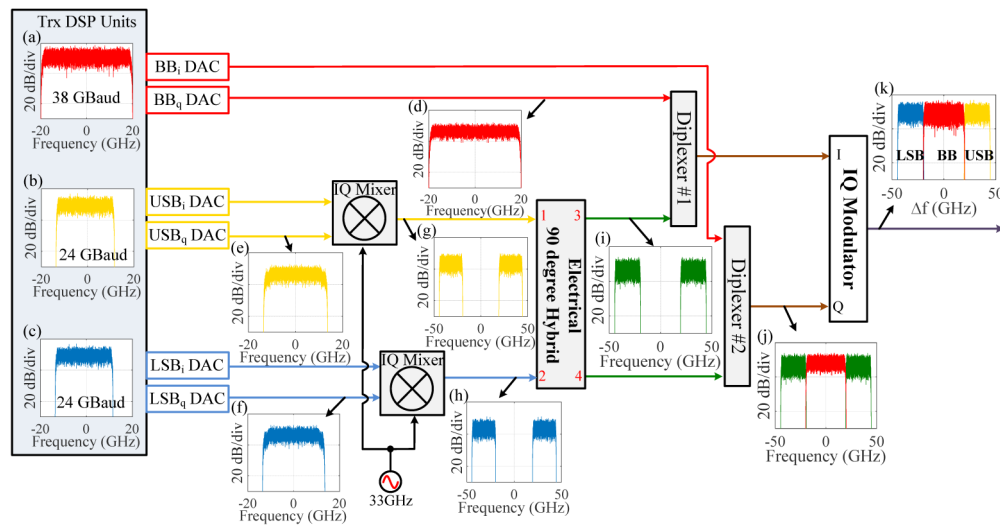


Fig. 1. Architecture of the proposed SCM-based 86-GBaud signal generation.

An electrical four-port 90 degree hybrid is then used to perform Hilbert transform on the two up-converted signals and signal combination at the output, i.e. $S_1 + \text{Hilbert}(S_2)$ at port 3 and $S_2 + \text{Hilbert}(S_1)$ at port 4, where S_1 and S_2 represent the signals input to port 1 and 2 respectively. As shown in Fig. 1(i), two up-converted signals are jointly combined through the hybrid. The output signal and its Hilbert transform are separately combined with the in-phase and quadrature of the 38-GBaud baseband signal through two diplexers (each implementing a low-pass and a high-pass filter combination) before inputting to the IQ modulator. Comparing Figs. 1(j) with 1(k), we observe that the electrical 90 degree hybrid coupled with the IQ modulator suppresses the optical images of both LSB and USB, and allows independent data carried by LSB and USB, which is known as TSSB modulation.

2.2 TSSB modulation and residual RF local oscillator suppression

The principle of TSSB modulation based on an ideal electrical 90 degree hybrid has been described mathematically in [13], where infinite single sideband (SSB) suppression ratios (i.e. the power ratio between the desired optical SSB signal and its image) for both up-converted signals are achieved. However, the imperfections of the deployed commercial 90 degree hybrid [14] (with specified amplitude and phase imperfections of 1 dB and 5° respectively) together with the imbalance and non-ideal biases of the IQ modulator result in poor image suppression. As shown in Fig. 2(a), the measured SSB suppression ratios for symmetrically located LSB and USB are only 14.5 dB and 15 dB respectively, which can cause severe sub-band crosstalk within the generated TSSB signal, and therefore, degrade the overall system performance. The hybrid imperfection impact and a proposed solution to combat this problem will be discussed in Section 4.

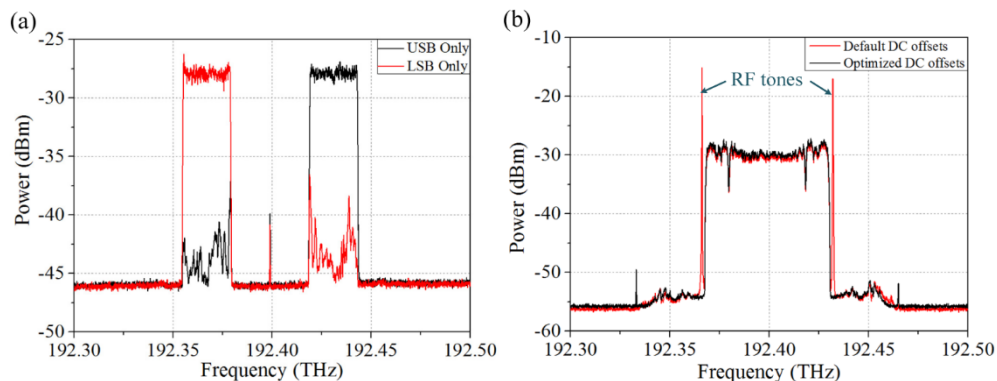


Fig. 2. Optical spectrum of (a) only one up-converted signal input to the electrical 90 degree hybrid, (b) the combined BB signal and -14-GHz digitally frequency shifted LSB and USB signals at default (0 V) and optimized DC offsets of the arbitrary waveform generator.

To ensure good conversion efficiency, both 33-GHz RF oscillators are power amplified to ~ 17.2 dBm before input to the IQ mixers. However, DC offsets and finite isolation between the LO and RF ports induced by balun imbalance and diode mismatch in the IQ mixers lead to carrier feedthrough. As observed during experimental demonstration, the residual RF tones within the up-converted signals resulted in unstable operation of the polarization de-rotation equalizer and led to OSNR penalty, making their suppression necessary to achieve optimized system performance. Adjusting DC offsets of the arbitrary waveform generator (AWG) induces imbalance in the diodes, which counteracts the intrinsic balun imbalance and improves the LO-RF isolation, resulting in suppression of residual RF carrier. This is similar to the way that DC biases applied to an optical Mach-Zehnder modulator overcomes intrinsic sub-arm imbalance. To illustrate the achieved suppression level, we digitally frequency shifted the 24-GBaud data by -14 GHz before the IQ mixers so that the generated optical LSB and USB signals can be separated from the residual RF tones, and then optimized output DC offsets of the AWG (Keysight M8195A). Figure 2(b) shows that the residual RF oscillators are suppressed by ~ 40 dB with optimal DC offsets.

2.3 Digital pre-emphasis

To compensate for the frequency roll-off of DACs, RF components and optical IQ modulator, digital pre-emphasis based on the receiver-side time-domain adaptive equalization [15] was implemented in the 86-GBaud transmitter. To calibrate for each band signal, we utilized intradyne detection at maximum available optical signal-to-noise ratio (OSNR), and employed four 43-tap T/2 spaced adaptive finite impulse response (FIR) filters with complex-valued weights optimized through the radius-directed algorithm after Fast Fourier transform (FFT)

based frequency offset compensation [16]. Following calibration, the achieved filter weights were applied to each band signal at 2 Samples/symbol in the transmitter. Figure 3 shows the measured inverse channel response for each spectral slice (averaged over ten measurements) by employing the receiver-side time-domain equalizer. We can see that the detected LSB signal in Fig. 3(a) suffers from larger attenuation at higher frequencies (over 8 GHz), which is opposite to the detected USB signal (frequencies less than -8 GHz) in Fig. 3(c) as expected. This can be attributed to the limited high passband (21.5-40 GHz) of the diplexer, since the up-converted 24-Gbaud electrical signals were centered at ± 32 GHz, occupying spectrum from 19.4 GHz to 44.6 GHz and from -44.6 GHz to -19.4 GHz. By contrast, ~ 5.4 -dB spectral attenuation is observed for the BB signal, which results from the uncompensated Sinc response of the DACs. The magnitude of the frequency response for all the three sub-channels is within ± 3 dB over the signal bandwidth, which can be compensated in the transmitter-side DSP. Figure 4 shows that the expected Nyquist shaped profiles have been achieved with digital pre-equalization separately performed for each sub-channel signal. The performance improvement brought about by digital pre-emphasis will be discussed in Section 4.

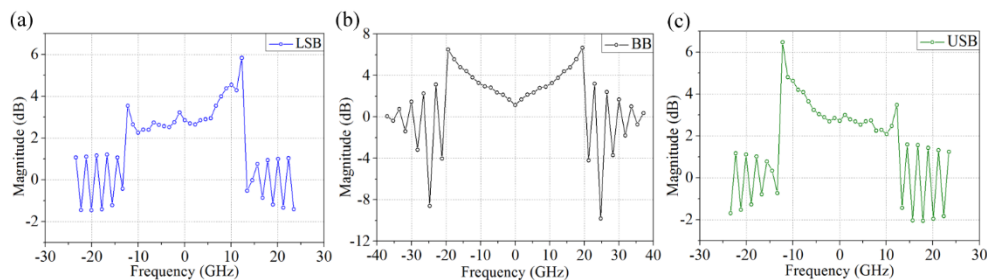


Fig. 3. Magnitude response of the receiver-side 43-tap adaptive equalizer for channel estimation of (a) LSB, (b) BB and (c) USB.

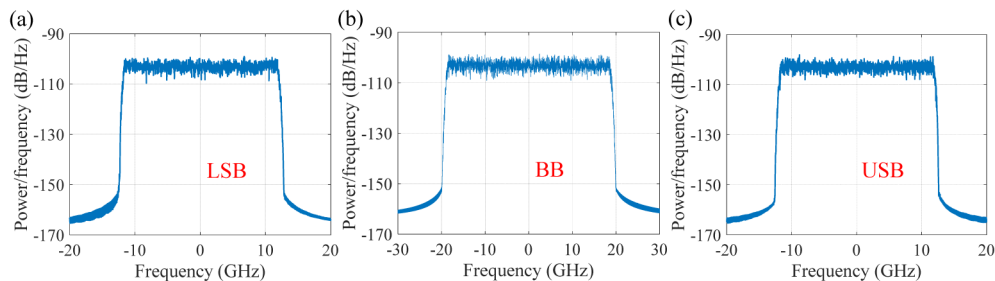


Fig. 4. Power spectral density of the detected (a) LSB, (b) BB and (c) USB signals.

3. Experimental setup

Figure 5 shows the experimental setup for the 86-Gbaud signal generation. In the DSP units for LSB and USB, independent $2^{15}-1$ pseudo random binary sequences (PRBSs) were firstly generated before differential bit encoding [17] implemented to mitigate cycle slips. After symbol mapping, the signals were up-sampled to 2 Samples/symbol and then Nyquist pulse shaped with 0.05 square root raised cosine filters. Digital pre-emphasis [Figs. 3(a) and 3(c)] based on the receiver-side adaptive equalizer was separately implemented for each band signal. After resampling to 64 GSa/s, the 24-Gbaud signals for the LSB and USB were digitally frequency shifted by -1 GHz with IQ skew compensated afterwards. Negative digital frequency shifts push the generated optical LSB and USB signals towards the BB signal, i.e. reduce the guard bands between the BB and LSB/USB, at a cost of increased sub-channel crosstalk. The -1 -GHz digital frequency shift employed in our system is decided by

trading off between the spectral efficiency and sub-channel crosstalk. The in-phase and quadrature components generated in LSB and USB DSP units were loaded to the AWG's memory and converted to analogue signals. Power amplified 33-GHz RF oscillators and two electrical passive IQ mixers (Marki Microwave, MLIQ-1845) with DC-20 GHz for baseband and 18-45 GHz for RF oscillator were employed for signal up-conversion. A broadband 2×2 electrical passive 90 degree hybrid [14] with frequency range of 5-50 GHz was utilized to perform the Hilbert transform and signal combination in the electrical domain. The two output signals of the hybrid were synchronized by adjusting two broadband RF phase shifters (LS-PI65-VFVM).

In the BB DSP Unit, every PRBS sequence was appended with one zero bit to make the symbol length to be a power of 2 so that resampling to match AWG granularity requirements is not needed. Similar DSP steps were performed except no digital frequency shift was introduced to the 38-GBaud baseband signal sampled at 76 GSa/s. The in-phase and quadrature components of the 38-GBaud signal were separately combined with the two up-converted signals through two diplexers [18] (specified low-pass band of DC-17 GHz and high-pass band of 21.5-40 GHz) before two 55-GHz bandwidth and 23-dB gain electrical amplifiers (SHF S807B). The amplified signals were finally modulated to the optical carrier (center frequency of 192.4 THz and linewidth of ~ 100 kHz) through an optical IQ modulator (Oclaro HB PM-QMZM) with 6-dB bandwidth of 45 GHz biased at null points.

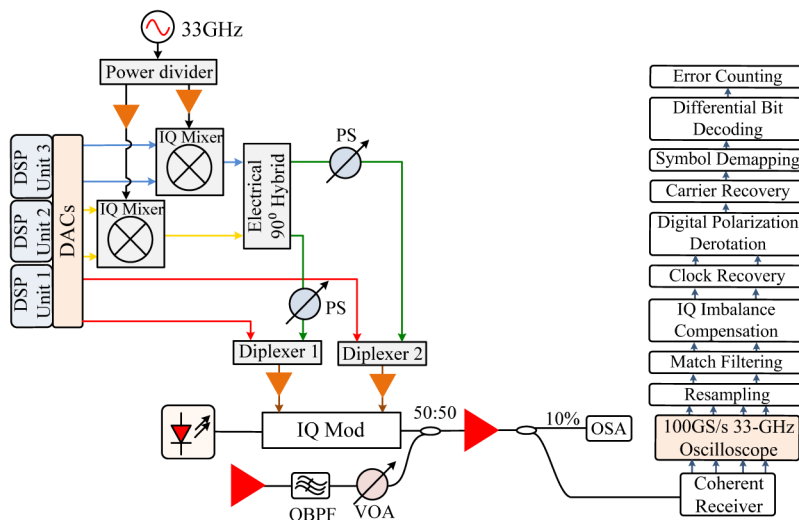


Fig. 5. Experimental setup for the 86-GBaud 16QAM system. PS: phase shifter; OBPF: optical bandpass filter; VOA: variable optical attenuator; OSA: optical spectrum analyzer.

Due to limited analogue bandwidth (33 GHz) and sampling rate (100 GSa/s) of the oscilloscope (Tektronix DPO77002SX), each spectral slice of the generated 86-GBaud 16QAM signal was detected separately by tuning the local oscillator to the center of each band. A high-resolution (150 MHz) optical spectrum analyzer (OSA) and the spectral integration method [19] with an integration bandwidth of 144 GHz were used for OSNR measurement. Due to slight nonlinearity in the OSA power measurement, an independently calibrated linearity correction factor (0.978) was applied to all measured OSNRs. The data captured at 100 GSa/s was firstly resampled to 2 Samples/symbol before matched filtering, which was implemented with square root raised cosine filters (roll-off factor of 0.05 and center frequency equal to the estimated frequency offsets). After IQ imbalance compensation and clock recovery, four 25-tap adaptive finite impulse response filters with tap spacing half of the symbol duration and complex-valued weights optimized through a radius-directed algorithm were utilized for digital polarization de-rotation. A FFT based frequency offset

compensator [16] and a blind phase search algorithm based phase estimator [20] were used for carrier recovery. After symbol decisions on the recovered data, differential bit decoding was performed on the resulting bit streams. The bit error rate (BER) for the 86-GBaud signal was calculated by summing up all the bit errors of three sub-channel signals over the total bit length.

4. Results and discussion

We firstly measured the OSNR performance for each individual band signal to verify the performance improvement brought by digital pre-emphasis. As shown in Fig. 6(a), the LSB signal behaves similarly to the USB signal in both cases (with and without digital pre-equalization). Compensating for the frequency roll-off in the transmitter reduces the required OSNR penalty at 7% HD-FEC threshold by 1.1 dB and 1.3 dB for the LSB and USB signals respectively. Compared with the theory of 24-GBaud differential bit encoded 16QAM (named D16QAM in the legend), the implementation penalty at BER of 3.8×10^{-3} is only 1 dB for both LSB and USB. By contrast, Fig. 6(b) shows that the 38-GBaud BB signal suffers from 3.1-dB implementation penalty without digital pre-emphasis. A performance improvement of 1.5 dB is observed for BB with digital pre-compensation for the frequency roll-off.

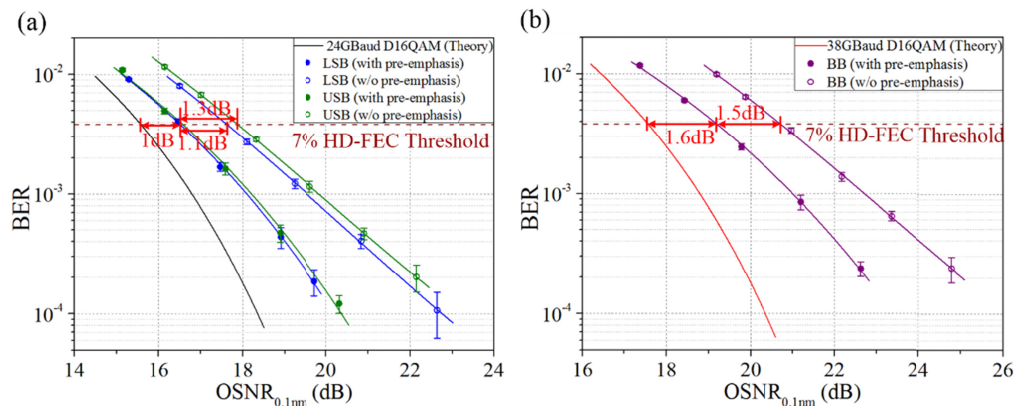


Fig. 6. OSNR performance of (a) 24-GBaud LSB and USB signals, (b) 38-GBaud BB signal with and without digital pre-emphasis. 16QAM with differential bit encoding (named D16QAM in the legends) was used for all the signals.

Electrically combining the three sub-channels together generates an 86-GBaud (aggregate symbol rate) signal with optical bandwidth of 88.7 GHz [see Fig. 7(a)], resulting in a spectral density of ~ 3.6 b/s/Hz/polarization. Measured BER performance of the high baud rate signal is depicted in Fig. 7(b), where a 6.2-dB implementation penalty at BER of 3.8×10^{-3} is observed. The inset constellation for each band signal at OSNR of 33 dB indicates that the overall system performance is mainly limited by the crosstalk between LSB and USB signals, which is discussed in detail below.

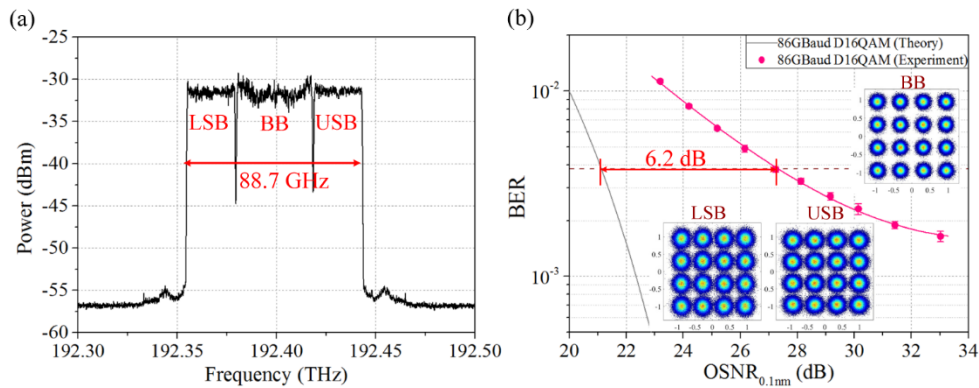


Fig. 7. (a) Optical spectrum of the 86-Gbaud differential bit encoded 16QAM signal. (b) Experimental OSNR performance of the 86-Gbaud SCM 16QAM signal with inset constellations for each recovered sub-channel signal at 33-dB OSNR.

In the case of single subcarrier signal input to only one port of the electrical 90 degree hybrid, which generates the desired optical SSB signal and its suppressed optical image [see Fig. 2(a)], the image signal power does not significantly affect the performance of the desired SSB signal, as indicated by the small implementation penalty of 1 dB for only LSB or USB in Fig. 6. However, when two subcarrier signals are fed into the electrical hybrid simultaneously, the residual optical images result in sideband crosstalk between LSB and USB, leading to large OSNR penalty. This poor image suppression can be attributed to the electrical 90 degree hybrid imperfections, imbalance and non-ideal biases of the IQ modulator. However, to evaluate the impact of hybrid imperfection on SSB suppression ratio, an ideal IQ modulator was utilized in the simulation. As shown in Fig. 8, an ideal hybrid allows SSB suppression ratio over 60 dB, which is reduced to 27 dB if the two output ports of the hybrid have 5° phase imperfection. In the case of only 1-dB amplitude difference, a smaller SSB suppression ratio of 18.2 dB is observed, which is quite close to the case with both impairments. This indicates that the amplitude balance of the electrical hybrid has larger impact on the SSB suppression ratio, consistent with our previous simulation results [13].

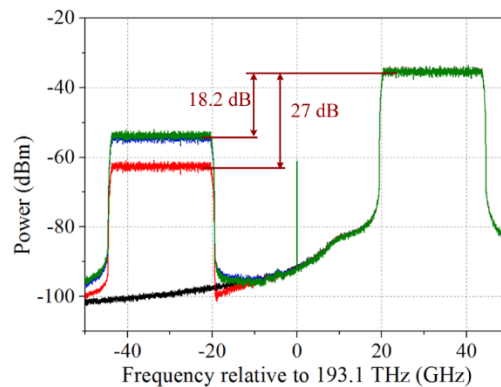


Fig. 8. Optical spectrum in the case of only USB signal using ideal hybrid (black) or imperfect hybrid with only 1-dB amplitude imbalance (blue), only 5° phase imperfection (red) or both impairments (green).

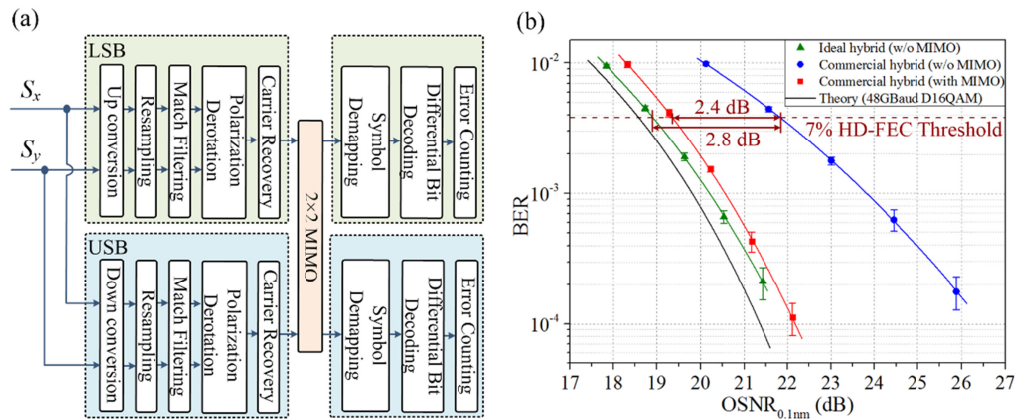


Fig. 9. (a) Receiver-side DSP flows and (b) OSNR performance of the simulated single polarization 48-GBaud TSSB signal detected by single 70-GHz full-band receiver in the case of ideal or imperfect electrical 90 degree hybrid with/without 31-tap 2×2 MIMO equalizer.

Since the 86-GBaud system performance is mainly limited by the sideband crosstalk between LSB and USB, we numerically studied the impact of hybrid imperfection on a single polarization 48-GBaud TSSB system (i.e. excluding the 38-GBaud BB signal) using either an ideal hybrid or an imperfect hybrid with both amplitude balance of 1 dB and phase imperfection of 5° . The generated LSB and USB signals with center frequency 32 GHz away from the optical carrier were simultaneously detected by a 70-GHz coherent receiver. Receiver-side DSP flows for the simulated single polarization 48-GBaud TSSB signal detected with single 70-GHz coherent receiver are shown in Fig. 9(a), where an optional 2×2 real-valued MIMO equalizer [21] based on the DDLMS algorithm was performed after carrier recovery for sideband crosstalk mitigation. As shown in Fig. 9(b), the performance of the 48-GBaud TSSB signal generated using the ideal 90 degree hybrid is close to theory with ~ 0.3 -dB OSNR penalty at 7% HD-FEC threshold. By contrast, the use of imperfect electrical 90 degree hybrid without MIMO further increases the penalty by 2.8 dB, which yet is reduced by 2.4 dB with the help of the 31-tap 2×2 MIMO post-equalizer. The resulted performance is only 0.4 dB worse than that using the ideal hybrid.

In the pol-mux case, a 4×4 MIMO equalizer instead of two 2×2 MIMO equalizers will be required to mitigate sub-band crosstalk within the TSSB signal. To verify the feasibility, we numerically investigated the performance of a dual-polarization 48-GBaud TSSB system in the case of ideal or the imperfect electrical hybrid with the receiver-side DSP flows shown in Fig. 10(a). We can see from Fig. 10(b) that hybrid imperfection results in an OSNR penalty of 3 dB at 7% HD-FEC threshold compared with the case using ideal electrical 90 degree hybrid. However, the 4×4 MIMO equalizer effectively alleviates the sub-band crosstalk impact and reduces OSNR penalty by 2.3 dB, which is similar to the performance improvement in Fig. 9(b) brought by the 2×2 MIMO post-equalizer in single polarization case.

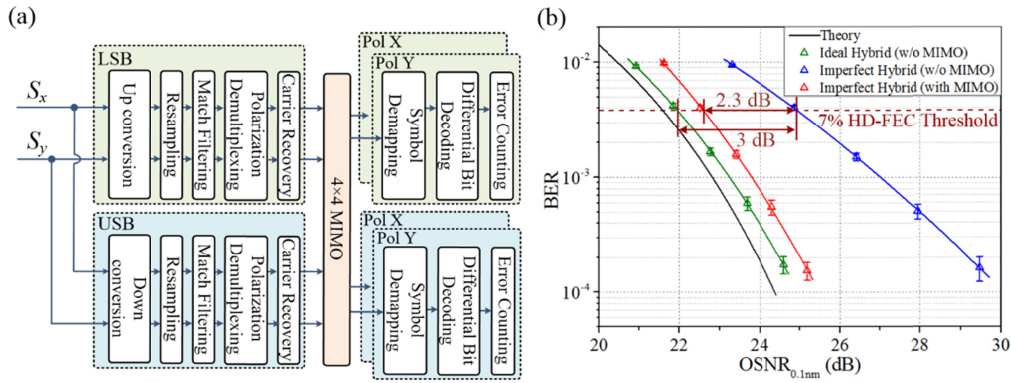


Fig. 10. (a) Receiver-side DSP flows and (b) OSNR performance of the simulated dual-polarization 48-GBaud TSSB signal detected by single 70-GHz full-band receiver in the case of ideal or imperfect electrical 90 degree hybrid with/without 31-tap 4×4 MIMO equalizer.

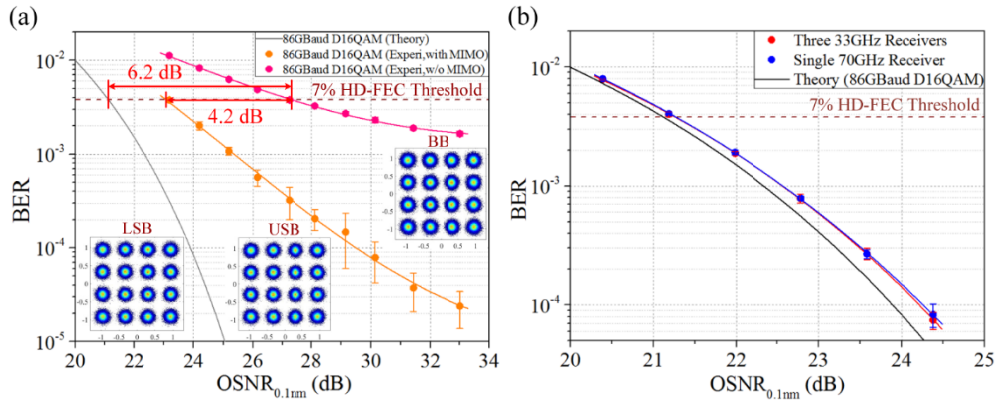


Fig. 11. (a) OSNR performance of the 86-GBaud 16QAM experimental system with/without 31-tap MIMO equalizer. Inset constellations are for each sub-channel signal recovered with MIMO equalizer at 33-dB OSNR. (b) Simulated OSNR performance of the 86-GBaud SCM 16QAM numerical system using single 70-GHz 200-GSa/s coherent receiver (blue dots) or three 33-GHz 100-GSa/s coherent receivers (red dots) in the case of ideal electrical 90 degree hybrid.

We subsequently experimentally demonstrated the benefit of such a MIMO post-equalizer for sideband crosstalk mitigation. Since the received signals were separately detected, sideband synchronization between the phase recovered LSB and USB signals was performed before the 31-tap MIMO post-equalizer. It can be seen from Fig. 11(a) that the MIMO post-equalizer improves the performance of the 86-GBaud 16QAM signal by 4.2 dB, giving an implementation penalty of only 2 dB with respect to theory. Such performance improvement can be also validated by comparing the inset constellations for LSB and USB in Fig. 7(b) and Fig. 11(a) at the same OSNR of 33 dB. Similar to the implementation of digital pre-emphasis in our scheme, pre-compensation for the sideband crosstalk can be also performed in the transmitter by applying the MIMO equalizer weights on the 24-GBaud signals at 1 Sample/symbol.

Considering that sub-band detection was utilized in our system due to limited analogue bandwidth (33 GHz) and sampling rate (100 GSa/s) of the oscilloscope, we numerically investigated the performance of single polarization 86-GBaud SCM signal using single 70-GHz 200-GSa/s coherent receiver for full band detection or three 33-GHz 100-GSa/s coherent receivers for sub-band detection. Since ideal electrical 90 degree hybrid was utilized in simulation, the post MIMO equalizer was deactivated. For full-band detected LSB and USB,

the associated DSP flows were the same as that in Fig. 9(a), while up/down conversion was eliminated from the DSP for full-band detected BB and also for the three individually detected sub-band signals. As shown in Fig. 11(b), practically the same performance is observed, indicating negligible performance difference between detection methods.

We note that an 86-GBaud 16QAM signal can be directly generated using only high-speed DACs such as DAC-II in [9]. The data rate of such systems can be further increased using the proposed scheme with higher frequency RF components, and the proposed mixed signal technique with parallel signal processing also potentially reduces power consumption [22]. Despite discrete high-frequency RF components utilized in our system architecture, implementations based on monolithic microwave integrated circuit (MMIC) technology are possible, which coupled with digital pre-emphasis for bandwidth limitation compensation and post-MIMO equalization for sideband crosstalk (within TSSB signal) mitigation will enable consistent system performance. Since only single polarization back-to-back performance is experimentally investigated in this paper, fiber transmission performance of dual-polarization 86-GBaud SCM 16QAM signal will be studied in our future work.

5. Conclusion

We have proposed and experimentally demonstrated a SCM-based high baud rate signal generation using passive RF components and single IQ modulator. The use of electrical 90 degree hybrid and IQ modulator allows TSSB modulation without requiring joint digital signal combination in the transmitter, simplifying the transmitter-side DSP to be only pulse shaping and digital pre-emphasis. Digital pre-emphasis based on the receiver-side adaptive equalizer enables OSNR performance improvement of 1.1 dB, 1.3 dB and 1.5 dB for each individual LSB, USB and BB signal respectively at 7% HD-FEC threshold. Furthermore, the implementation penalty of the joint 86-GBaud 16QAM signal is only 2 dB thanks to the 31-tap MIMO post-equalizer for sideband crosstalk mitigation.

Funding

The Engineering and Physical Sciences Research Council projects PEACE (EP/L000091/1), UPON (EP/M005283/1), SPFS (EP/L00044X/1), TOM3 (EP/M009092/1).

Acknowledgments

We thank Oclaro for providing the large-bandwidth IQ modulator used in our experimental demonstration, and the author T. Zhang acknowledges financial support from China Scholarship Council.

References

1. E. Torrenco, R. Cigliutti, G. Bosco, G. Gavioli, A. Alaimo, A. Carena, V. Curri, F. Forghieri, S. Piciaccia, M. Belmonte, A. Brinciotti, A. La Porta, S. Abrate, and P. Poggiolini, "Transoceanic PM-QPSK Terabit superchannel transmission experiments at Baud-rate subcarrier spacing," in Proceedings of IEEE European Conference and Exhibition on Optical Communication (IEEE, 2010), pp. 1–3.
2. F. C. G. Gunning, T. Healy, and A. D. Ellis, "Dispersion tolerance of coherent WDM," *IEEE Photonic Tech. L.* **18**(12), 1338–1340 (2006).
3. M. Huang, A. Tanaka, E. Ip, Y. Huang, D. Qian, Y. Zhang, S. Zhang, P. N. Ji, I. B. Djordjevic, T. Wang, Y. Aono, S. Murakami, T. Tajima, T. J. Xia, and G. A. Wellbrock, "Terabit/s Nyquist Superchannels in High Capacity Fiber Field Trials Using DP-16QAM and DP-8QAM Modulation Formats," *J. Lightwave Technol.* **32**(4), 776–782 (2014).
4. X. Zhou and L. E. Nelson, "400G WDM Transmission on the 50 GHz Grid for Future Optical Networks," *J. Lightwave Technol.* **30**(24), 3779–3792 (2012).
5. R. Rios-Müller, J. Renaudier, P. Brindel, H. Mardoyan, P. Jennevé, L. Schmalen, and G. Charlet, "1-Terabit/s net data-rate transceiver based on single-carrier Nyquist-shaped 124 GBaud PDM-32QAM," in Optical Fiber Communication Conference Post Deadline Papers, OSA Technical Digest (online) (Optical Society of America, 2015), paper Th5B.1.
6. H. Mardoyan, R. Rios-Müller, M. A. Mestre, P. Jennevé, L. Schmalen, A. Ghazisaeidi, P. Tran, S. Bigo, and J. Renaudier, "Transmission of Single-Carrier Nyquist-Shaped 1-Tb/s Line-Rate Signal over 3,000 km," in Optical

- Fiber Communication Conference, OSA Technical Digest (online) (Optical Society of America, 2015), paper W3G.2.
7. J. Zhang, J. Yu, and N. Chi, "Transmission and full-band coherent detection of polarization-multiplexed all-optical Nyquist signals generated by Sinc-shaped Nyquist pulses," *Sci. Rep.* **5**(1), 13649 (2015).
 8. H. Yamazaki, M. Nagatani, S. Kanazawa, H. Nosaka, T. Hashimoto, A. Sano, and Y. Miyamoto, "Digital-preprocessed analog-multiplexed DAC for ultra-wide-band multilevel transmitter," *J. Lightwave Technol.* **34**(7), 1579–1584 (2016).
 9. H. Chien, J. Yu, Y. Cai, B. Zhu, X. Xiao, Y. Xia, X. Wei, T. Wang, and Y. Chen, "Approaching Terabits per Carrier Metro-Regional Transmission Using Beyond-100GBd Coherent Optics with Propabilistically Shaped DP-64QAM Modulation," *J. Lightwave Technol.*
 10. A. Narasimha, X. J. Meng, M. C. Wu, and H. Chien, "WDM Transmission of Single-Carrier 120-GBd ETDM PDM-16QAM Signals Over 1200-km Terrestrial Fiber Links," *J. Lightwave Technol.* **35**(4), 1033–1040 (2017).
 11. X. Chen, S. Chandrasekhar, S. Randel, G. Raybon, A. Adamiecki, P. Pupalakis, and P. J. Winzer, "All-Electronic 100-GHz Bandwidth Digital-to-Analog Converter Generating PAM Signals up to 190 GBaud," *J. Lightwave Technol.* **35**(3), 411–417 (2017).
 12. A. Narasimha, X. J. Meng, M. C. Wu, and E. Yablonovitch, "Tandem single sideband modulation scheme for doubling spectral efficiency of analogue fibre links," *Electron. Lett.* **36**(13), 1135–1136 (2000).
 13. T. Zhang, C. Sanchez, S. Sygletos, I. Phillips, and A. Ellis, "Amplifier-free 200-Gb/s tandem SSB doubly differential QPSK signal transmission over 80-km SSMF with simplified receiver-side DSP," *Opt. Express* **26**(7), 8418–8430 (2018).
 14. Available at <http://www.markimicrowave.com/Assets/datasheets/QH-0550.pdf>.
 15. J. Zhang, J. Yu, N. Chi, and H. C. Chien, "Time-domain digital pre-equalization for band-limited signals based on receiver-side adaptive equalizers," *Opt. Express* **22**(17), 20515–20529 (2014).
 16. Y. Wang, K. Shi, and E. Serpedin, "Non-Data-Aided Feedforward Carrier Frequency Offset Estimators for QAM Constellations: A Nonlinear Least-Squares Approach," *EURASIP J. Adv. Sig. Pr.* **2004**(2004), 856139 <https://doi.org/10.1155/S1110865704403175>.
 17. W. Weber, "Differential Encoding for Multiple Amplitude and Phase Shift Keying Systems," *IEEE Trans. Commun.* **26**(3), 385–391 (1978).
 18. Available at <https://www.markimicrowave.com/Assets/datasheets/DPX-1721.pdf>.
 19. Available at <https://www.viavisolutions.com/en-us/literature/band-osnrmeasurements-40-g-polarization-multiplexed-qpsk-signals-using-fielddeploy-white-paper-en.pdf>.
 20. T. Pfau, S. Hoffmann, and R. Noe, "Hardware-Efficient Coherent Digital Receiver Concept With Feedforward Carrier Recovery for M-QAM Constellations," *J. Lightwave Technol.* **27**(8), 989–999 (2009).
 21. S. Fan, Q. Zhuge, Z. Xing, K. Zhang, T. M. Hoang, M. Morsy-Osman, M. Y. S. Sowailam, Y. Li, J. Wu, and D. V. Plant, "264 Gb/s Twin-SSB-KK Direct Detection Transmission Enabled by MIMO Processing," in *Optical Fiber Communication Conference, OSA Technical Digest (online)* (Optical Society of America, 2018), paper W4E.5.
 22. R. Brennan and T. Schneider, "An ultra low-power DSP system with a flexible filterbank," *Conference Record of Thirty-Fifth Asilomar Conference on Signals, Systems and Computers (Cat.No.01CH37256)*, Pacific Grove, CA, USA, 2001, pp. 809–813.